

# Effect of Coulomb Stress on the Gutenberg-Richter Law for the Seismicity after the Landers Earthquake

Víctor Navas-Portella,<sup>1,2,3</sup> Abigail Jiménez,<sup>4</sup> and Álvaro Corral<sup>1,2,5,6</sup>

<sup>1</sup>*Centre de Recerca Matemàtica, Edifici C,  
Campus Bellaterra, E-08193 Barcelona, Spain*

<sup>2</sup>*Barcelona Graduate School of Mathematics, Edifici C,  
Campus Bellaterra, E-08193 Barcelona, Spain*

<sup>3</sup>*Facultat de Matemàtiques i Informàtica,  
Universitat de Barcelona, Barcelona, Spain*

<sup>4</sup>*Departamento de Computación e Inteligencia Artificial. Universidad de Granada. Campus Ceuta C/. Cortadura del Valle s.n., 51001 Ceuta, Spain*

<sup>5</sup>*Departament de Matemàtiques, Universitat  
Autònoma de Barcelona, E-08193 Barcelona, Spain*

<sup>6</sup>*Complexity Science Hub Vienna, Josefstädter Straße 39, 1080 Vienna, Austria*

## Abstract

Coulomb-stress theory has been used for years in seismology to understand how earthquakes trigger each other. Whenever an earthquake occurs, the stress field changes, and places with positive increases are brought closer to failure. Earthquake models that relate earthquake rates and Coulomb stress after a main event, such as the rate-and-state model, assume that the distribution of earthquake magnitudes is not affected by the change in the Coulomb stress. We apply several statistical analyses to the aftershock sequence of the Landers earthquake (California, USA, 1992, moment magnitude 7.3), to show that the distribution of magnitudes is sensitive to the sign of the Coulomb-stress increase; in particular, the  $b$ -value of the Gutenberg-Richter law is significantly decreased for events that received a decrease in the Coulomb stress. These events have a distribution of focal mechanisms very close to the one of the previous-to-mainshock seismicity, whereas the events with a positive increase of the stress are characterized by a much larger proportion of strike-slip events.

---

## INTRODUCTION

Since the L'Aquila event in 2009 seismologists have advocated the modeling and testing of earthquakes within a rigorous statistical framework [26], following on the CSEP (Collaboratory for the Study of Earthquake Predictability) previous works. A recent pseudo-prospective forecast was conducted on the 2010-2012 Canterbury, New Zealand, series, in order to test a total of fourteen earthquake models [38, 64]. Its results offer some encouragement for a physical basis in earthquake forecasting and suggest that some of the recent physics-based and hybrid model development has added informative components [5].

Our basic understanding of earthquake physics is that stress is being accumulated on certain regions due to different mechanisms, and that those regions rupture whenever that stress surpasses the strength of the material. That rupture is the earthquake. The mechanisms by which stresses change are diverse: in addition to tectonic driving, they can be induced by precedent earthquakes [32, 39, 55, 57], by volcanic activity [50], or even by artificial means, such as injection of fluids or aquifer withdrawal [52]. Coulomb-stress theory has been used to forecast spatial patterns of aftershock rates. Although there exist instances where its predictive skills are arguable [14, 18, 34, 35], the monitoring of the changes in the stress field represents a valuable information for seismic and volcanic hazard forecasting and to proposing the adequate mitigation measures. A hallmark of statistical seismology and of earthquake hazard assessment is the well-known Gutenberg-Richter relation, or Gutenberg-Richter law [17, 28, 60]. This law states that earthquake magnitudes must be described in terms of a probability distribution and that, above a lower cut-off value, this distribution is exponential. In terms of the probability density  $f(m)$  one has

$$f(m) = (b \ln 10) 10^{-b(m-m_{min})} \propto 10^{-bm},$$

defined for  $m \geq m_{min}$  (values below  $m_{min}$  are disregarded), with  $m$  the magnitude (moment magnitude in our case),  $m_{min}$  the lower cut-off in magnitude,  $b$  the so called  $b$ -value (directly related to the exponent  $\beta$  of the power-law distribution of seismic moment,  $1 + \beta = 2b/3$ ), and the symbol  $\propto$  denoting proportionality. A straightforward property of the exponential distribution leads to the fact that the rate (the number per unit time of earthquakes above a certain magnitude  $m$ ) is also a decreasing exponential function of the magnitude, with the same  $b$ -value.

---

Earthquake hazard forecasts usually comprise two stages: in the first one, the rate of events is forecasted, while in the second one, the Gutenberg-Richter law is applied to those rates in order to obtain the probabilities of occurrence for each magnitude threshold. In the case of physics-based models, the forecasted rates of events depend on the Coulomb stresses calculated in the region of interest. These models are variants of the rate-and-state model by Dieterich [12],

$$R(t) = r [1 + (e^{-\Delta CFS/B} - 1) e^{-t/t_a}]^{-1} \quad (1)$$

where  $R(t)$  is the rate of events (i.e., aftershocks) at any given time  $t$  after a mainshock,  $r$  is the rate of background seismicity,  $\Delta CFS$  is the increase in Coulomb stress induced by the mainshock,  $B$  is the combination of two constitutive parameters, and  $t_a$  is the characteristic relaxation time [12].

Note that in the application of the Gutenberg-Richter law to the forecasted rate  $R(t)$  given by the previous expression is implicit that the Coulomb-stress change caused by a mainshock does not alter the fulfillment of the Gutenberg-Richter law for the aftershocks, in particular, this law remains the same no matter if  $\Delta CFS$  is positive or negative. In some sense,  $R(t)$  inherits the dependence of the background rate  $r$  with the magnitude. Therefore, the rate-and-state formulation [3, 4, 6, 12, 44, 58] assumes the fulfillment of the Gutenberg-Richter law for the incoming events (aftershocks), with no change in the  $b$ -value. This assumption is made when inverting earthquake rates to obtain stress changes [13, 49, 50]. Physics-based models also assume the magnitude distribution does not depend on the stress values, so that forecasted rates can be translated into probabilities of occurrence for different magnitudes.

In fact, it has been long debated [29] whether the value of  $b$  in the Gutenberg-Richter law is essentially universal or whether, on the contrary, it is affected by different geophysical conditions. Some studies [40, 48] have correlated the  $b$ -value (and also the parameters of the Omori law [43, 59, 61]) with the style of faulting. These studies indicate that (at least for California)  $b \approx 1.03$  for normal events,  $b \approx 0.87$  for strike-slip events, and  $b \approx 0.79$  for thrust events [48]. As the  $b$ -value is directly related to the log-ratio between the number of small and large earthquakes, variations in  $b$  can be associated with the ability of an earthquake rupture to propagate (more large events, low  $b$ ) or not (less large events, high  $b$ ).

According to Mohr-Coulomb theory [31, 40], thrust faults rupture at much higher stress than normal faults (with strike-slip faults in between, assuming the same value for the coefficient of static friction). When the stress required to initiate a rupture is higher, stress inter-

---

actions are enhanced and cracks can propagate faster in many different directions, yielding larger earthquakes [40], consistent with the empirically observed  $b$ -values for thrust faulting [48]. Conversely, for lower rupture thresholds, one should find indeed the large  $b$ -values characterizing normal faulting. Although the threshold for triggering might be different for the different styles of faulting, the rupture or not of a fault also depends on its previous state. Moreover, when calculating the stress induced by previous events (mainshocks) on new events (aftershocks) it is necessary to orientate it onto the fault [24, 37], so that one can actually evaluate if the new events could have been triggered by the induced stress or not.

Here we investigate, with rigorous statistical tools, if the Gutenberg-Richter law is affected by the binary choice between positive and negative increases of the Coulomb stress, using the sequence of events after the Landers (1992) earthquake. The next section explains the seismic catalog and the spatio-temporal window used to define this sequence. Section 3 develops the procedure to calculate the increase in the Coulomb stress that the Landers earthquake provokes in the fault plane of each event in the sequence. The statistical analysis is also exposed in this section. Section 4 presents the results and Sec. 5 summarizes the conclusions.

## DATA

The June 28, 1992, Landers earthquake, with a moment magnitude  $m = 7.3$  and a rake angle  $\rho = -177^\circ$ , corresponding to strike-slip focal mechanism, has been the strongest one in southern California at least since 1952. The earthquake and its subsequent aftershock sequence have been extensively studied [15, 19, 22], with a number of slip distributions that describe its rupture [21, 54, 63]. The slip model we will use here is the one in Ref. [63]. High quality catalogs for southern California are nowadays available [20, 30]; in particular in this paper we will select the Landers' aftershocks from the Yang-Hauksson-Shearer (YHS) catalog [66], which incorporates focal-mechanism solutions. This, together with Landers stress field derived from the slip model, allows us to calculate Coulomb-stress increases (positive or negative) provoked by the Landers event (the mainshock) on the actual orientations of the aftershock ruptures.

In order to better detect the influence of the Landers stress change we take a time window

---

of 100 days after the Landers mainshock and a spatial window reaching 150 km from the Landers rupture. Events closer than 5 km to the rupture zone will be also excluded; the reason is the undetermination of the deformation field near the edges of the subfaults [42], as the finite-fault approximation provides spurious values near the fault zone. This spatio-temporal window define Landers aftershocks for our purposes. Although we tried other choices for the limits of the window, the used one, selected “a priori” supported by basic aftershock knowledge, turned out to be the one that maximized the effect of the Landers mainshock on the difference of  $b$ -values for the aftershocks under positive and negative Coulomb-stress increase.

## PROCEDURE

The dMODELS software of Ref. [2] calculates the deformation field (or displacement) caused by different models corresponding to different physical processes. Although there exist many programs that calculate deformation caused by earthquakes, this package has been thoroughly tested, and can introduce many different sources of deformation, which can be translated into stress changes in a straightforward way.

The local coordinate system for dMODELS is east-north-up, ENU. After introducing the corresponding slip model (also called source model) for the mainshock of interest (Landers in our case [63]) we obtain the projections in the ENU axes of the deformation field  $\vec{u}$  caused by the mainshock at the position of each aftershock (and also at its neighborhood, in order to take derivatives). We then obtain the strain tensor associated to  $\vec{u}$  by calculating the (symmetrized) gradient of the deformation [33], whose components are  $\varepsilon_{ij} = (\nabla_i u_j + \nabla_j u_i)/2$  (with a spatial step equal to 1 km).

Afterwards, we assume an isotropic and elastic material for calculating the stress tensor [33], or, more precisely, the contribution of the mainshock to the stress tensor,  $s_{ij} = 2\mu\varepsilon_{ij} + \lambda\delta_{ij} \sum_k \varepsilon_{kk}$ , with  $\delta_{ij}$  the components of the identity matrix and with the Lamé elastic moduli given by  $\mu = \lambda = 3 \times 10^4$  MPa [31]. Given the fault plane and slip vector of an aftershock, we calculate the change in the normal  $\sigma_n$  and shear (or tangential)  $\tau$  stresses in that orientation and position, as

$$\Delta\sigma_n = \sum_{ij} n_i s_{ij} n_j \text{ and } \Delta\tau = \sum_{ij} \ell_i s_{ij} n_j, \quad (2)$$

with  $n_i$  and  $\ell_i$  the components of the normal and slip vectors, respectively. The formulas

---

to obtain the ENU components of these vectors from the information recorded in the YHS catalog (strike, dip and rake angles) are given in the Methods section. Note that in order to be realistic, the Coulomb-stress changes have to be calculated onto the planes of the actual faults [37]. This contrasts with an approach in which Coulomb stresses are calculated onto the so-called optimally oriented planes [32], when the only information available is the regional stress.

The Mohr-Coulomb failure criterion [62] states that the shear stress  $\tau$  on a fault that ruptures must surpass the critical value  $\tau_c$ , which is a linear function of the normal stress,

$$\tau_c = C - \mu' \sigma_n \quad (3)$$

with  $C$  the cohesion and  $\mu'$  the effective fault friction coefficient (including the contribution of the pore pressure [8, 32]). Care must be taken with the convention of signs in the normal stress, which is not the same in geophysics than in solid mechanics (our convection takes the negative sign for compression). From this failure criterion it is natural to define the Coulomb stress as  $CFS = \tau + \mu' \sigma_n$ , which signals failure by  $CFS > C$ . Thus, the change in Coulomb stress at the aftershock fault plane due to the mainshock will be

$$\Delta CFS = \Delta \tau + \mu' \Delta \sigma_n, \quad (4)$$

with  $\Delta \tau$  and  $\Delta \sigma_n$  coming from Eq. (2). Thus, positive increases of the Coulomb stress bring the fault closer to failure, whereas negative increases distance it away from failure. As the real value of the effective friction coefficient  $\mu'$  is uncertain [31], we will perform our study for different values of it,  $\mu' = 0.2, 0.4, 0.6$ , and  $0.8$ , as in Ref. [18]. The complete procedure to obtain the Coulomb stress is summarized in Fig. 1.

Once we know the Coulomb-stress change in the fault plane of each aftershock we can separate these attending to the value of the change, with the most natural separation being between positive and negative increases (denoted by sub-indexes  $>$  and  $<$ , respectively). Naturally, we expect to obtain many more aftershocks with positive increases than with negative ones [56]. It is for each of these subsets that we will study the fulfilment of the Gutenberg-Richter law.

For any set or subset (or sub-catalog) of earthquakes, the value of  $b$  in the Gutenberg-Richter law can be automatically obtained by maximum-likelihood estimation, as

$$b = \frac{\log_{10} e}{\bar{m} - m_{min}} \quad (5)$$

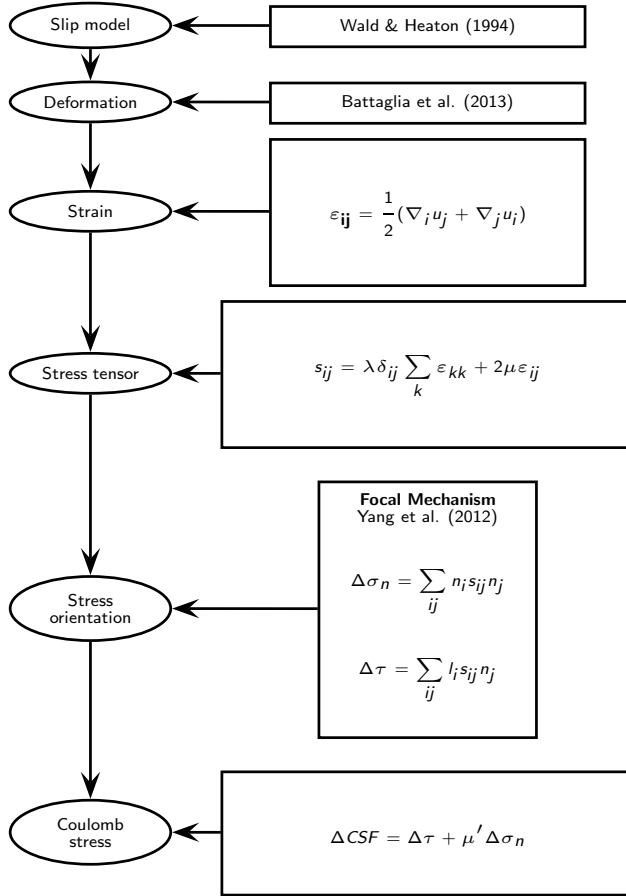


FIG. 1. Flowchart summarizing the procedure to obtain the Coulomb stress on each aftershock fault plane from the slip model and the focal-mechanism catalog.

[1, 36], with  $\bar{m}$  the mean magnitude of the events considered (i.e., those above  $m_{min}$ ). Let us stress that  $m_{min}$  is not the minimum magnitude recorded in the catalog but the value from which we fit the Gutenberg-Richter law to the data.

In principle, results should not significantly depend on the value of  $m_{min}$ , but the larger its value the less data to calculate the  $b$ -value and the larger the uncertainty, whereas for a too small  $m_{min}$  the Gutenberg-Richter law would not be fulfilled due to the incompleteness of the catalog and the resulting  $b$ -value would be artefactual. In this paper we have taken  $m_{min} = 3$ , which ensures the fulfilment of the Gutenberg-Richter law for all data sets analysed, as we have verified by means of the Kolmogorov-Smirnov goodness-of-fit test [46], where the distribution of the test statistic and, from it, the  $p$ -value of the fit,  $p_{fit}$ , is calculated using  $10^4$  Monte Carlo simulations [7, 11]. Although some fitting procedures look

---

for the value of  $m_{min}$  that optimizes the fit for a given data set [7, 11], we have opted for a fixed  $m_{min}$  in order to compare the different subsets on the same footing. So, in all cases the exponential fit for  $m \geq 3$  cannot be rejected ( $p$ -value of the test larger than 0.05). Note that  $m_{min}$  defined in this way can be considered a magnitude of completeness, and thus, our value of  $m_{min}$  turns out to be rather conservative, in the sense that it is larger (and therefore safer) than in other works [65].

The maximum-likelihood estimation of the  $b$ -value has an associated uncertainty given by its standard deviation

$$\sigma = \frac{b}{\sqrt{N}},$$

where  $N$  is the number of earthquakes with  $m \geq m_{min}$  in the subset, out of a total number  $N_{tot}$  (of any magnitude). Note that this uncertainty only depends on the number of data, and has nothing to do with the goodness of the fit. This result, as well as the formula for the maximum-likelihood estimation of  $b$ , Eq. (5), can be obtained from Ref. [11] just taking into account the relation between moment magnitude and seismic moment.

The comparison between the  $b$ -values of the subsets with different values of  $\Delta CFS$  is done by means of the following statistic

$$z = \frac{b_{>} - b_{<}}{\sqrt{\sigma_{>}^2 + \sigma_{<}^2}} = \frac{b_{>} - b_{<}}{\sqrt{b_{>}^2/N_{>} + b_{<}^2/N_{<}}},$$

where the sub-indexes  $>$  and  $<$  refer to positive and negative increases of the Coulomb stress. This statistics is rooted on the null hypothesis that both subsets of data (positive and negative) belong to the same underlying population of earthquake magnitudes and then, both estimators of the  $b$ -value ( $b_{>}$  and  $b_{<}$ ) have a common mean value, which is that of the whole population. Therefore, under the null hypothesis,  $b_{>} - b_{<}$  has zero mean and standard deviation  $\sqrt{\sigma_{>}^2 + \sigma_{<}^2}$  (approximating the population variance from the sample values of  $b_{>}$  and  $b_{<}$  and assuming zero covariance between  $b_{>}$  and  $b_{<}$ ) and then  $z$  has zero mean too and unit standard deviation.

An additional assumption is that  $z$  is normally distributed, which is supported by theory in the asymptotic limit ( $N_{>}$  and  $N_{<}$  going to infinity [45]). Assuming normality we will test the null hypothesis just comparing the value of  $z$  with the standard normal distribution and the hypothesis will be rejected if the value of  $z$  is too extreme for a given significance level; in quantitative terms this will be given by a  $p$ -value, called  $p_{norm}$ , smaller than the significance level (0.05, let us say; corresponding to 0.95 confidence).

---

If we do not want to believe that the asymptotic regime has been reached the best option is to use a permutation test [16]. Under the null hypothesis (all values of magnitude belong to the same population) one is allowed to aggregate both subsets (positive and negative) and take, without repetition, two sub-samples of size  $N_>$  and  $N_<$ ; note that this is equivalent to take a permutation of the aggregated sample and separate it into two parts ( $>$  and  $<$ ). One proceeds in the same way as in the original data, calculating (by maximum likelihood)  $b_>^*$ ,  $b_<^*$ , and from here  $\sigma_>^*$ ,  $\sigma_<^*$ , and  $z^*$ , where the asterisk marks that we are dealing with a permutation of the original data. Repeating the permutation procedure many times we find the distribution of  $z^*$ , which can be compared with the original value  $z$ . The  $p$ -value of the permutation test,  $p_{perm}$ , will be given by the fraction of permutations for which  $|z^*|$  is larger than  $|z|$  (the empirical value). In our case we take  $10^4$  permutations.

## RESULTS

Table I shows the results of applying the previous procedure to the Landers aftershock sequence. We can see how, in the overall case (when events are not separated in terms of Coulomb-stress change), the Gutenberg-Richter law is fulfilled with  $b_{all} = 0.88 \pm 0.03$ , with the uncertainty corresponding to just one standard deviation. This  $b$ -value for the Landers aftershocks is found, not surprisingly, to be close to the average for aftershocks in California,  $b \simeq 0.9$  [25, 47], and somewhat below the long-term value of southern California (all events),  $b \simeq 1.0$  [23] (although other works report  $b \simeq 1.0$  for Landers aftershocks, probably due to the consideration there of a much smaller magnitude of completeness [51]).

After separating by the sign of the Coulomb-stress change, the first result that becomes apparent from the table is that the number of aftershocks with positive increases is much larger (about a factor five) than the number for the negative case [32, 55], no matter the value of  $\mu'$  used to calculate  $\Delta CFS$ . Regarding the  $b$ -values, although they depend slightly on  $\mu'$ , we can summarize them as  $b_> \simeq 0.91 \pm 0.04$  and  $b_< \simeq 0.73 \pm 0.08$ . Note that the magnitude distribution for the overall case is a mixture of the distributions corresponding to  $\Delta CFS > 0$  and  $\Delta CFS < 0$ , and therefore, the value of  $b$  in the overall case turns out to be the harmonic mean of  $b_>$  and  $b_<$ , i.e.,

$$b_{all}^{-1} = \frac{N_>b_>^{-1} + N_<b_<^{-1}}{N_> + N_<}, \quad (6)$$

---

see Ref. [41]. If instead of  $\Delta CFS > 0$  we consider  $\Delta CFS > 0.1$  MPa, the resulting values of  $b$  are nearly the same, but with a larger uncertainty,  $b_{>0.1} \simeq 0.90 \pm 0.045$  (with little dependence on the value of  $\mu'$ ). Despite of the fact the values of  $b_{>}$  and  $b_{<}$  look different between them (and also the values of  $b_{>0.1}$  and  $b_{<}$ ), with an apparent decrease for the negative increase of the Coulomb stress ( $\Delta CFS < 0$ ), statistical testing becomes necessary in order to establish significance [9].

Table II compares  $b_{>}$  and  $b_{<}$ , and shows that for the central values of  $\mu'$  (0.4 and 0.6, which are the more realistic) the difference in the  $b$ -values can be considered significantly different from zero with a confidence larger than 95% ( $p$ -values around 0.045, close to but smaller than 0.05); so,  $b_{>} \neq b_{<}$ . For the more extreme values of  $\mu'$  the rejection of the null hypothesis of equality is not so clear:  $\mu' = 0.2$  is in the limit of rejection and  $\mu' = 0.8$  is not reaching rejection (with a 95% confidence level). For the comparison between the cases  $\Delta CFS > 1$  MPa and  $\Delta CFS < 0$ , the fact that the uncertainty of  $b_{>0.1}$  is larger than that of  $b_{>}$  (despite the values themselves are rather similar) leads to a non-significant difference between  $b_{>0.1}$  and  $b_{<}$ , and we cannot reject that  $b_{>0.1} \simeq b_{<}$ .

As a complement, instead of the fitted  $b$ -values we may directly compare the distributions; this can be done with the two-sample Kolmogorov-Smirnov test, whose null hypothesis is that both data sets come from the same population, so, the two empirical distributions ( $>$  and  $<$ ) are two realizations of a unique theoretical distribution (which remains unveiled) [46]. Restricting again to magnitudes larger than 3 the resulting  $p$ -values of this test ( $p_{2ks}$ ) for different values of  $\mu'$  turn out to be smaller than 0.05, and therefore significant, which confirms that the distributions for positive and negative  $\Delta CFS$  are different with a 95 % confidence, see Table II.

A different comparison comes from the application of the Akaike information criterion ( $AIC$ ). We consider that we aggregate both subsets (positive and negative  $\Delta CFS$ ) but keeping the distinction in the sign of  $\Delta CFS$ . Then, we contemplate two options. Model 1, simple: we fit the aggregated data set with one single Gutenberg-Richter exponential (in fact, we have already done that, leading to the value  $b_{all}$  in Table I). Model 2, “complex”: we fit each data set with its own exponential function (values  $b_{>}$  and  $b_{<}$  in the same table). In each case,  $AIC = 2k - 2\hat{\ell}$ , where  $k$  is the number of parameters of each model and  $\hat{\ell}$  is the log-likelihood of the model at maximum. The model yielding the smallest  $AIC$  should be preferred. Computing the difference,  $\Delta AIC = AIC_2 - AIC_1 = 2 - 2(-22867.42 + 22869.27) =$

---

−1.7; so, the “complex” model 2, with two separate  $b$ -values, is preferred in front the simplicity of just one  $b$ -value (on the other hand, a likelihood-ratio test does not find enough evidence in favor of the complex model; this is not contradictory as this test is more strict than the  $AIC$ ).

As mentioned in the introduction, some authors have unveiled a direct dependence of the  $b$ -value on the focal mechanism of the events, which implies a dependence of  $b$  on the total stress (not the stress increase) [48]. Table I includes, for the same data set, the effect of the values of the rake angle  $\rho$  on the  $b$ -value. The rake angle is associated to the focal mechanism in the following way: values of the rake around  $-90^\circ$  correspond to normal events (labelled as  $no$ ), values around  $0^\circ$  or  $\pm 180^\circ$  to strike-slip events ( $ss$ ), and values around  $90^\circ$  to thrust events ( $th$ ).

In contrast to the results of our Coulomb-stress study, we do not find any significant effect of the rake on the  $b$ -value, due to the low number of events in the normal and thrust regimes (which increases the uncertainty). The results are  $b_{no} \simeq 0.98 \pm 0.13$ ,  $b_{ss} \simeq 0.87 \pm 0.04$ , and  $b_{th} \simeq 0.89 \pm 0.20$ , see Table I. But despite the large uncertainty, the values of  $b_{no}$  and  $b_{ss}$  are in agreement with the results of Ref. [48]; however, our value of  $b_{th}$  turns out to be rather large in comparison (but compatible, within the error bars).

We could try to explain the value of the difference in the  $b$ -values between the earthquakes with  $\Delta CFS > 0$  and  $\Delta CFS < 0$  in terms of differences in focal mechanisms between the two populations; for instance, writing  $b_{>}$  as a function of  $b_{no}$ ,  $b_{ss}$ , and  $b_{th}$ , using the analogous of Eq. (6). However, we do not find well defined values of the latter when each of these is splitted into a contribution from  $\Delta CFS > 0$  and another one from  $\Delta CFS < 0$ , i.e., we do not find  $b_{>no} \simeq b_{<no} \simeq b_{no}$ , etc., see Table III.

Instead, it seems that it is the sign of the Coulomb-stress increase which primary determines the value of  $b$ , and not the focal mechanism, with the value of  $b$  showing little dependence on the latter, for a fixed sign of the Coulomb-stress increase, i.e.,  $b_{>no} \simeq b_{>ss} \simeq b_{>th} \simeq b_{>} \simeq 0.9$  to  $1.0$  and  $b_{<no} \simeq b_{<ss} \simeq b_{<th} \simeq b_{<} \simeq 0.72$  to  $0.76$  (despite the large uncertainty). We note that all “composite” values of  $b$  in Table III (marginal rows and columns) verify the law of harmonic means, Eq. (6).

From this law, and the values of  $b_{no}$ ,  $b_{th}$ ,  $b_{>}$ , and  $b_{<}$ , we conclude that the ratio  $N_{>no}/N_{<no}$  is higher than  $N_{>th}/N_{<th}$ ; i.e., in normal events the contribution from  $\Delta CFS > 0$  is higher than in thrust events, as can be verified looking at Table III. The contribution from  $\Delta CFS >$

---

0 to strike-slip events ( $N_{>ss}/N_{<ss}$ ) is even higher (see the table again), but this cannot be anticipated from the harmonic-mean law, due to the fact that the value of  $b_{>ss}$  is not close enough to the values of  $b_{>no}$  and  $b_{>th}$ , and one cannot take a common value for them in the comparisons of the strike-slip events with the other events.

Comparing with the number of earthquakes with each focal mechanism for the 5 years previous to Landers ( $N_{no} = 77$ ,  $N_{th} = 61$ , and  $N_{ss} = 498$  for  $m > 3$ ) we conclude that it is indeed the low number of thrust aftershocks with positive  $\Delta CFS$  which is anomalous (and not the relatively high number of them for negative  $\Delta CFS$ ), due to an increase in the number of normal events and an even higher increase in strike-slip events triggered ( $\Delta CFS > 0$ ) by the Landers mainshock. This difference in numbers becomes visually apparent in Fig. 3. Although the two populations ( $\Delta CFS > 0$  and  $< 0$ ) are different in terms of focal mechanism, there is no substantial difference in the fulfilling of the Omori law. Indeed, if we compare this for the two subsets we find the “characteristic” power-law Omori decay of the rate with very similar values of the Omori exponent. Note that this is in disagreement with the rate-and-state formulation [12].

## DISCUSSION

We have seen how the positive Coulomb-stress increase associated to the Landers mainshock triggered a very large number of strike-slip events and also a large number of normal events, but much less thrust events. Although this result seems easy to establish, as it can be obtained without the calculation of  $\Delta CFS$  (due to the fact that most of the events have  $\Delta CFS > 0$  and thus, this subset dominates the overall statistics), we have unambiguously associated these events to the positive  $\Delta CFS$ . Moreover, these events have  $b$ -values that are in the usual range, between 0.9 and 1.0.

On the other side, the events in the opposite regime (with  $\Delta CFS < 0$ ) keep a proportion between normal, strike-slip, and thrust events rather different to the  $\Delta CFS > 0$  case, and close to that of the immediately previous record (1989-1992, up to Landers). The  $b$ -values of these events turn out to be anomalous (too low), close to 0.74, with very little dependence on the focal mechanism. These results are also largely independent on the value  $\mu'$  used to calculate the change in Coulomb stress. It is a curious fact that this  $b$ -value corresponds very closely to the power-law exponent of a critical branching process (the so-called mean-

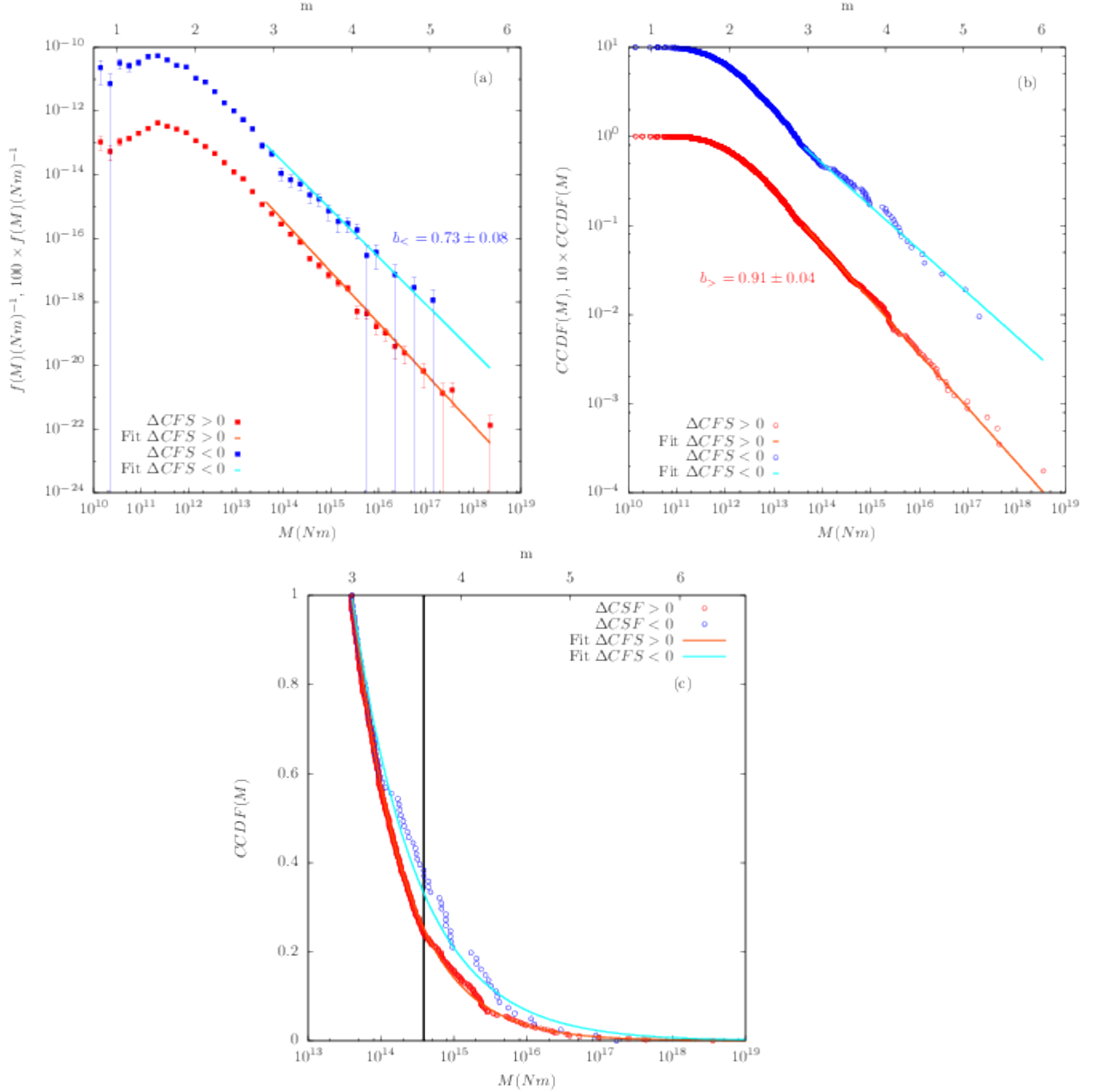


FIG. 2. Estimation of the probability densities (a) and of the complementary cumulative distribution functions (CCDF) (b) and (c) of seismic moment  $M$  for Landers aftershocks with  $\Delta CFS > 0$  and  $\Delta CFS < 0$ , using  $\mu' = 0.4$  in the calculation of  $\Delta CFS$ . (b) and (c) contain essentially the same information, displayed in different ways. Curves corresponding to  $\Delta CFS < 0$  have been conveniently multiplied by a factor in (a) and (b) for clarity sake. A vertical line in (c) denotes where the Kolmogorov-Smirnov statistic is attained.

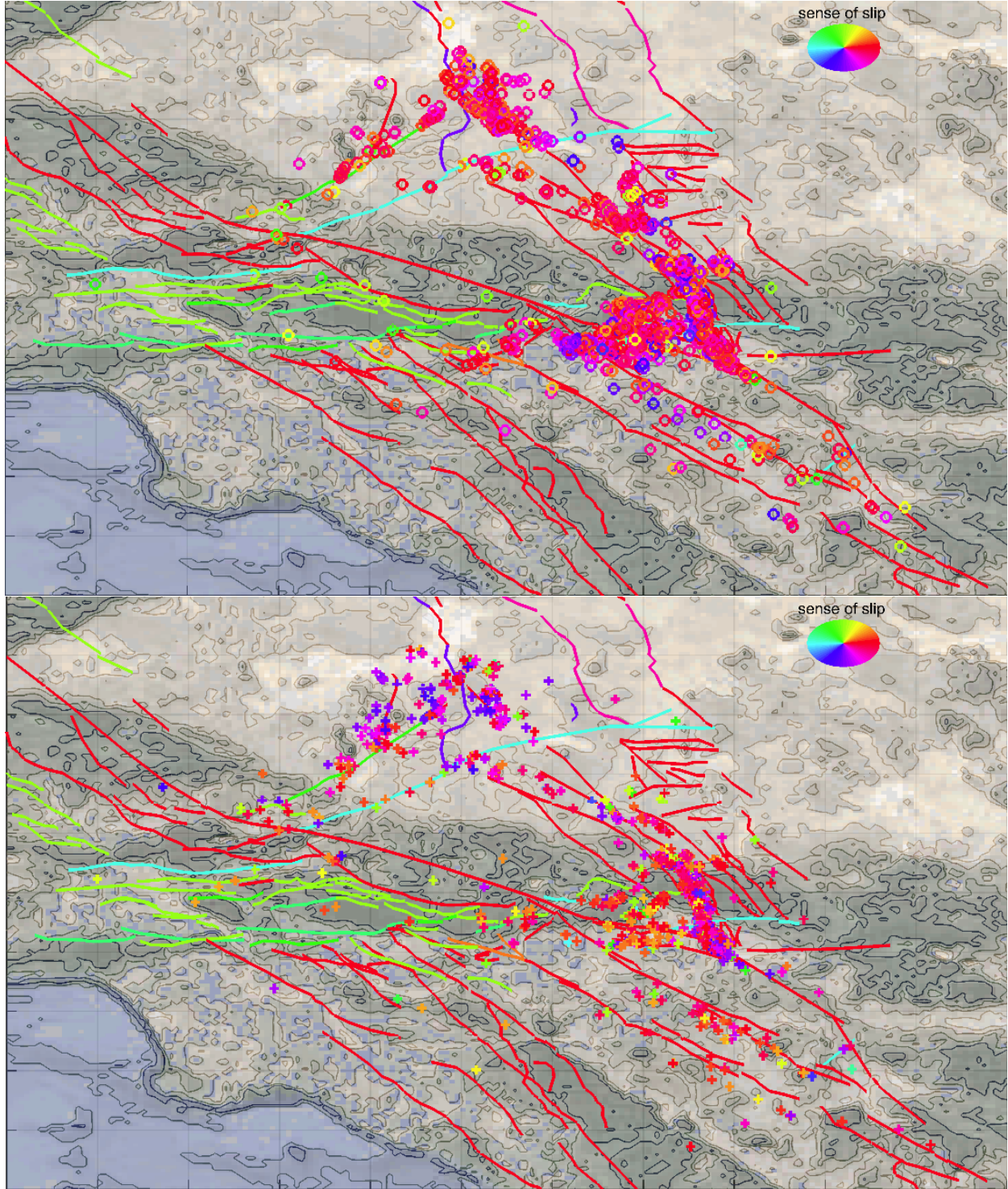


FIG. 3. Rakes of Landers aftershocks compared to the fault network (time window of 100 days after the mainshock). Top:  $\Delta CFS > 0$ . Bottom:  $\Delta CFS < 0$ . Color scale for the sense of slip: red for right-lateral ( $\rho$  close to  $\pm 180^\circ$ ), light blue for left-lateral ( $\rho$  close to  $0^\circ$ ), green for normal ( $\rho$  close to  $-90^\circ$ ) and dark blue or purple for thrust faulting ( $\rho$  close to  $90^\circ$ ). No restriction on the magnitude values is used. An area of  $550 \times 500$  km is shown.

	$N_{tot}$	$N$	$b$ -value	$\sigma$	$p_{fit}$
Overall	6730	662	$b_{all} = 0.882$	0.034	$0.233 \pm 0.004$
$\mu' = 0.2, \Delta CFS > 0$	5632	573	$b_{>} = 0.900$	0.038	$0.255 \pm 0.004$
$\Delta CFS < 0$	1098	89	$b_{<} = 0.739$	0.078	$0.321 \pm 0.005$
$\mu' = 0.4, \Delta CFS > 0$	5678	580	$b_{>} = 0.909$	0.038	$0.267 \pm 0.004$
$\Delta CFS < 0$	1052	82	$b_{<} = 0.729$	0.081	$0.617 \pm 0.005$
$\mu' = 0.6, \Delta CFS > 0$	5670	582	$b_{>} = 0.909$	0.038	$0.264 \pm 0.004$
$\Delta CFS < 0$	1060	80	$b_{<} = 0.730$	0.082	$0.416 \pm 0.005$
$\mu' = 0.8, \Delta CFS > 0$	5603	583	$b_{>} = 0.906$	0.038	$0.263 \pm 0.004$
$\Delta CFS < 0$	1127	79	$b_{<} = 0.739$	0.083	$0.286 \pm 0.005$
$< 135^\circ \leq \rho \leq -45^\circ$	1227	56	$b_{no} = 0.976$	0.131	$0.580 \pm 0.005$
$45^\circ \leq \rho \leq 135^\circ$	302	20	$b_{th} = 0.886$	0.198	$0.985 \pm 0.005$
the rest	5201	586	$b_{ss} = 0.874$	0.036	$0.249 \pm 0.004$

TABLE I. Results of fitting the Gutenberg-Richter law to the Landers aftershocks, separating positive and negative Coulomb-stress increases, for different values of the effective friction coefficient  $\mu'$  and  $m_{min} = 3$ . The overall case (with  $\Delta CFS$  taking any sign) is also included and labelled as “all”. Aftershocks correspond to the first 100 days after the Landers mainshock. Distance of aftershocks to the Landers rupture is restricted to be between 5 and 150 km. The  $p$ -value of the goodness-of-fit test is computed with  $10^4$  simulations and is denoted by  $p_{fit}$ . Its uncertainty corresponds to one standard deviation.

field limit,  $1 + \beta_{<} = 1 + 2b_{<}/3 \simeq 1.49 \pm 0.05 \simeq 3/2$ ) [10]. It has been argued that this is the true value one should observe in general if it not were for a series of artifacts and biases in the measurement of earthquake sizes [27].

The difference of the  $b$ -values ( $b_{>} - b_{<}$ ) is close to the onset of statistical significance, due to the large uncertainties caused by the low number of events. Nevertheless, the two-sample Kolmogorov-Smirnov test supports the fact that the distributions of magnitudes with  $\Delta CFS$  above and below zero are different. Certainly, more research using other mainshocks (for which detailed slip models are available) is necessary. This will not only increase significance but will elucidate if the difference between  $b_{>}$  and  $b_{<}$  is a peculiarity of the Landers sequence or it can be a generic property of aftershocks.

$\mu'$	$z$	$p_{norm}$	$p_{perm}$	$d_{2ks}$	$p_{2ks}$
0.2	1.949	0.051	$0.0495 \pm 0.002$	0.156	0.041
0.4	2.029	0.042	$0.042 \pm 0.002$	0.159	0.046
0.6	1.991	0.046	$0.047 \pm 0.002$	0.170	0.030
0.8	1.834	0.067	$0.069 \pm 0.003$	0.176	0.024

TABLE II. Results of two statistical tests comparing magnitude distributions for positive and negative Coulomb-stress changes, using different values of  $\mu'$ . Columns 2 to 4: testing the null hypothesis that there is no difference between the  $b$ -values (i.e.,  $b_{>} = b_{<}$ ). Columns 5 to 6: testing the null hypothesis that there is no difference in the distributions, using the 2-sample Kolmogorov-Smirnov test. Same data as previous table. In the first test, both asymptotic normality of the  $z$  statistic and a permutation test are used for the calculation of the  $p$ -value (labeled as  $p_{norm}$  and  $p_{perm}$ , respectively). In the latter case the number of permutations is  $10^4$ , and the uncertainty of  $p_{perm}$  corresponds to one standard deviation.  $d_{2ks}$  and  $p_{2ks}$  are the Kolmogorov-Smirnov statistic and its  $p$ -value.

$fm$	$N_{>fm}$	$N_{<fm}$	$N_{fm}$	$b_{>fm}$	$b_{<fm}$	$b_{fm}$
No: $< 135^\circ \leq \rho \leq -45^\circ$	48	8	$N_{no} = 56$	1.024	0.762	$b_{no} = 0.976$
Th: $45^\circ \leq \rho \leq 135^\circ$	12	8	$N_{th} = 20$	1.018	0.742	$b_{th} = 0.886$
SS: the rest	520	66	$N_{ss} = 586$	0.898	0.724	$b_{ss} = 0.874$
Overall	580	82	$N_{all} = 662$	0.909	0.729	$b_{all} = 0.882$

TABLE III. Number of events and  $b$ -values corresponding to Landers aftershocks with  $m > 3$  separated by sign of the Coulomb-stress increase ( $>$  and  $<$ ) and by focal mechanism ( $fm$ ).  $fm = no$  (normal),  $ss$  (strike-slip), and  $th$  (thrust). The Coulomb stress is calculated with  $\mu' = 0.4$ . Same data as in previous tables. Compare also with the values previous to Landers ( $N_{no} = 77$ ,  $N_{th} = 61$ , and  $N_{ss} = 498$  for  $m > 3$ ).

Regarding the implications for physics-based models of aftershock sequences, these models assume the  $b$ -value in the Gutenberg-Richter law is constant for the whole aftershock zone. This is the foundation for both inverting stress from seismicity rates [13, 49, 50] and for forecasting the seismicity afterwards ([5] and references therein). However, our results demand for more complete models of aftershock occurrence in order to get better forecasts.

Not only different styles of faulting for the aftershocks should be acknowledged, but also the sign of the Coulomb-stress increase should lead to different parameterizations in the rate-and-state model.

## METHODS

The YHS catalog characterizes fault planes and slip vectors by means of three angles: strike  $\Theta$ , dip  $\delta$ , and rake  $\rho$ . In term of these, the normal vector of the fault is given by

$$\hat{n} = \begin{pmatrix} n_E \\ n_N \\ n_U \end{pmatrix} = \begin{pmatrix} \cos \Theta \sin \delta \\ -\sin \Theta \sin \delta \\ \cos \delta \end{pmatrix} \quad (7)$$

in the ENU coordinate system [53]. In the same way, the slip vector is obtained as

$$\hat{\ell} = \begin{pmatrix} \ell_E \\ \ell_N \\ \ell_U \end{pmatrix} = \begin{pmatrix} \sin \Theta \cos \rho - \cos \Theta \cos \delta \sin \rho \\ \cos \Theta \cos \rho + \sin \Theta \cos \delta \sin \rho \\ \sin \delta \sin \rho \end{pmatrix}. \quad (8)$$

Note that  $\hat{n}$  and  $\hat{\ell}$  are unit vectors.

- 
- [1] K. Aki, *Maximum likelihood estimate of b in the formula  $\log N = a - bm$  and its confidence limits*, Bull. Earthq. Res. Inst. Univ. Tokyo **43** (1965), no. 2, 237–239.
  - [2] M. Battaglia, P. F. Cervelli, and J. R Murray, *dMODELS: A MATLAB software package for modeling crustal deformation near active faults and volcanic centers*, J. Volcanol. Geotherm. Res. **254** (2013), 1 – 4.
  - [3] C. Cattania, S. Hainzl, L. Wang, B. Enescu, and F. Roth, *Aftershock triggering by postseismic stresses: A study based on Coulomb rate-and-state models*, J. Geophys. Res. **120** (2015), 2388–2407.
  - [4] C. Cattania, S. Hainzl, L. Wang, F. Roth, and B. Enescu, *Propagation of Coulomb stress uncertainties in physics-based aftershock models*, J. Geophys. Res. **119** (2014), 7846–7864.
  - [5] C. Cattania, M. J. Werner, W. Marzocchi, S. Hainzl, D. Rhoades, M. Gerstenberger, M. Liukis, W. Savran, A. Christophersen, A. Helmstetter, A. Jiménez, S. Steacy, and T. H. Jordan, *The*

- 
- forecasting skill of physics-based seismicity models during the 2010-2012 Canterbury, New Zealand, earthquake sequence*, Seism. Res. Lett. **89** (2018), no. 4, 1238.
- [6] C. H. Chan, Y. M. Wu, and J. P. Wang, *Earthquake forecasting through a smoothing kernel and the rate-and-state friction law: Application to the Taiwan region*, Nat. Hazards Earth Syst. Sci. **12** (2012), 1–13.
- [7] A. Clauset, C. R. Shalizi, and M. E. J. Newman, *Power-law distributions in empirical data*, SIAM Rev. **51** (2009), 661–703.
- [8] M. Cocco and J. R. Rice, *Pore pressure and poroelasticity effects in Coulomb stress analysis of earthquake interactions*, J. Geophys. Res.: Solid Earth **107** (2002), no. B2, ESE 2–1–ESE 2–17.
- [9] A. Corral, G. Boleda, and R. Ferrer-i-Cancho, *Zipf’s law for word frequencies: Word forms versus lemmas in long texts*, PLoS ONE **10** (2015), no. 7, e0129031.
- [10] A. Corral and F. Font-Clos, *Criticality and self-organization in branching processes: application to natural hazards*, Self-Organized Criticality Systems (M. Aschwanden, ed.), Open Academic Press, Berlin, 2013, pp. 183–228.
- [11] A. Deluca and A. Corral, *Fitting and goodness-of-fit test of non-truncated and truncated power-law distributions*, Acta Geophys. **61** (2013), 1351–1394.
- [12] J. Dieterich, *A constitutive law for rate of earthquake production and its application to earthquake clustering*, J. Geophys. Res.: Solid Earth **99** (1994), no. B2, 2601–2618.
- [13] J. Dieterich, V. Cayol, and P. Okubo, *The use of earthquake rate changes as a stressmeter at Kilauea volcano*, Nature **408** (2000), 457–460.
- [14] K. R. Felzer and E. E. Brodsky, *Testing the stress shadow hypothesis*, J. Geophys. Res.: Solid Earth **110**, no. B5.
- [15] J. Gomberg, P. A. Reasenberg, P. Bodin, and R. A. Harris, *Earthquake triggering by seismic waves following the Landers and Hector Mine earthquakes*, Nature **411** (2001), no. 6836, 462–466.
- [16] P. I. Good, *Resampling methods*, 3rd ed., Birkhäuser, Boston, 2011.
- [17] B. Gutenberg and C. F. Richter, *Frequency of earthquakes in California*, Bull. Seismol. Soc. Am. **34** (1944), 185–188.
- [18] J. L. Hardebeck, J. J. Nazareth, and E. Hauksson, *The static stress change triggering model: Constraints from two southern California aftershock sequences*, J. Geophys. Res. **103** (1998),

- 
- 24,427–24,437.
- [19] E. Hauksson, L. M. Jones, K. Hutton, and D. Eberhart-Phillips, *The 1992 Landers earthquake sequence: Seismological observations*, J. Geophys. Res.: Solid Earth **98** (1993), no. B11, 19835–19858.
- [20] E. Hauksson, W. Yang, and P. M. Shearer, *Waveform relocated earthquake catalog for Southern California (1981 to June 2011)*, Bull. Seismol. Soc. Am. **102** (2012), 2239–2244.
- [21] B. Hernandez, F. Cotton, and M. Campillo, *Contribution of radar interferometry to a two-step inversion of the kinematic process of the 1992 Landers earthquake*, J. Geophys. Res.: Solid Earth **104** (1999), no. B6, 13083–13099.
- [22] D. P. Hill, P. A. Reasenber, A. Michael, W. J. Arabaz, G. Beroza, D. Brumbaugh, J. N. Brune, R. Castro, S. Davis, D. dePolo, W. L. Ellsworth, J. Gomberg, S. Harmsen, L. House, S. M. Jackson, M. J. S. Johnston, L. Jones, R. Keller, S. Malone, L. Munguia, S. Nava, J. C. Pechmann, A. Sanford, R. W. Simpson, R. B. Smith, M. Stark, M. Stickney, A. Vidal, S. Walter, V. Wong, and J. Zollweg, *Seismicity remotely triggered by the magnitude 7.3 Landers, California, earthquake*, Science **260** (1993), no. 5114, 1617–1623.
- [23] K. Hutton, J. Woessner, and E. Hauksson, *Earthquake monitoring in southern California for seventy-seven years (1932-2008)*, Bull. Seismol. Soc. Am. **100** (2010), no. 2, 423.
- [24] T. Ishibe, Y. Ogata, H. Tsuruoka, and K. Satake, *Testing the Coulomb stress triggering hypothesis for three recent megathrust earthquakes*, Geosci. Lett. **4** (2017).
- [25] L. M. Jones, *Foreshocks, aftershocks, and earthquake probabilities: Accounting for the Landers earthquake*, Bull. Seismol. Soc. Am. **84** (1994), no. 3, 892.
- [26] T. H. Jordan, Y. T. Chen, P. Gasparini, R. Madariaga, I. Main, W. Marzocchi, G. Papadopoulos, G. Sobolev, K. Yamaoka, and J. Zschau, *Operational Earthquake Forecasting. State of knowledge and guidelines for utilization*, Annals of Geophysics **54** (2011).
- [27] Y. Y. Kagan, *Earthquake size distribution: Power-law with exponent  $\beta \equiv 1/2?$* , Tectonophys. **490** (2010), 103–114.
- [28] ———, *Earthquakes: Models, statistics, testable forecasts*, Wiley, 2014.
- [29] Y. Kamer and S. Hiemer, *Data-driven spatial b value estimation with applications to California seismicity: To b or not to b*, J. Geophys. Res. **120**, no. 7, 5191–5214.
- [30] Y. Kamer, G. Ouillon, D. Sornette, and J. Wössner, *Condensation of earthquake location distributions: Optimal spatial information encoding and application to multifractal analysis of*

- 
- South Californian seismicity*, Phys. Rev. E **92** (2015), 022808.
- [31] H. Kanamori and E. E. Brodsky, *The physics of earthquakes*, Rep. Prog. Phys. **67** (2004), 1429–1496.
- [32] G. King, R. S. Stein, and J. Lin, *Static stress changes and the triggering of earthquakes*, Bull. Seismol. Soc. Am. **84** (1994), 935–953.
- [33] B. Lautrup, *Physics of continuous matter*, 2nd ed., CRC Press, 2011.
- [34] E. P. Mallman and M. D. Zoback, *Assessing elastic Coulomb stress transfer models using seismicity rates in southern California and southwestern Japan*, J. Geophys. Res.: Solid Earth **112**, no. B3.
- [35] D. Marsan, *Triggering of seismicity at short timescales following Californian earthquakes*, J. Geophys. Res. **108** (2003), 1–14.
- [36] W. Marzocchi and L. Sandri, *A review and new insights on the estimation of the b-value and its uncertainty*, Annals of Geophysics **46** (2009), no. 6, 1271–1282.
- [37] J. McCloskey, S. S. Nalbant, S. Steacy, C. Nostro, O. Scotti, and D. Baumont, *Structural constraints on the spatial distribution of aftershocks*, Geophys. Res. Lett. **30** (2003), no. 12, 1610–1613.
- [38] A. J. Michael and M. J. Werner, *Preface to the focus section on the Collaboratory for the Study of Earthquake Predictability (CSEP): New results and future directions*, Seism. Res. Lett. **89** (2018), no. 4, 1226.
- [39] S. Nandan, G. Ouillon, J. Woessner, D. Sornette, and S. Wiemer, *Systematic assessment of the static stress triggering hypothesis using interearthquake time statistics*, J. Geophys. Res.: Solid Earth **121** (2016), 1890–1909.
- [40] C. Narteau, S. Byrdina, P. Shebalin, and D. Schorlemmer, *Common dependence on stress for the two fundamental laws of statistical seismology*, Nature **462** (2009), 642–645.
- [41] V. Navas-Portella, I. Serra, A. Corral, and E. Vives, *Increasing power-law range in avalanche amplitude and energy distributions*, Phys. Rev. E **97** (2018), 022134.
- [42] Y. Okada, *Internal deformation due to shear and tensile faults in a half-space*, Bull. Seismol. Soc. Am. **82** (1992), no. 2, 1018–1040.
- [43] F. Omori, *On the aftershocks of earthquakes*, Journal of the College of Science, Imperial University of Tokyo **7** (1894), 111–200.

- 
- [44] T. Parsons, S. Toda, R. S. Stein, A. Barka, and J. H. Dietrich, *Heightened odds of large earthquakes near Istanbul: An interaction-based probability calculation*, *Science* **288** (2000), 661–665.
- [45] Y. Pawitan, *In all likelihood: Statistical modelling and inference using likelihood*, Oxford UP, Oxford, 2001.
- [46] W. H. Press, S. A. Teukolsky, W. T. Vetterling, and B. P. Flannery, *Numerical recipes in FORTRAN*, 2nd ed., Cambridge University Press, Cambridge, 1992.
- [47] P. A. Reasenber and L. M. Jones, *Earthquake hazard after a mainshock in California*, *Science* **243** (1989), no. 4895, 1173–1176.
- [48] D. Schorlemmer, S. Wiemer, and M. Wyss, *Variations in earthquake-size distribution across different stress regimes*, *Nature* **437** (2005), 539–542.
- [49] L. Seeber and J. G. Armbruster, *Earthquakes as beacons of stress change*, *Nature* **407** (2000), 69–72.
- [50] P. Segall, A. L. Llenos, S.-H. Yun, A. M. Bradley, and E. M. Syracuse, *Time-dependent dike propagation from joint inversion of seismicity and deformation data*, *J. Geophys. Res.: Solid Earth* **118** (2013), no. 11, 5785–5804.
- [51] R. Shcherbakov, D. L. Turcotte, and J. B. Rundle, *Aftershock statistics*, *Pure Appl. Geophys.* **162** (2005), no. 6, 1051–1076.
- [52] M. Shirzaei, W. L. Ellsworth, K. F. Tiampo, P. J. González, and M. Manga, *Surface uplift and time-dependent seismic hazard due to fluid injection in Eastern Texas*, *Science* **353** (2016), no. 6306, 1416–1419.
- [53] D. E. Smith, *A new paradigm for interpreting stress inversions from focal mechanisms: how 3D stress heterogeneity biases the inversions toward the stress rate*, Ph.D. thesis, California Institute of Technology, 2006.
- [54] J. A. Spotila and K. Sieh, *Geologic investigations of a “slip gap” in the surficial ruptures of the 1992 Landers earthquake, southern California*, *J. Geophys. Res.* **100** (1995), 543–559.
- [55] S. Steacy, J. Gomberg, and M. Cocco, *Introduction to special section: stress transfer, earthquake triggering, and time-dependent seismic hazard*, *J. Geophys. Res.* **110** (2005), B05S01.
- [56] R. S. Stein, *The role of stress transfer in earthquake occurrence*, *Nature* **402** (1999), 605–609.
- [57] R.S. Stein, G.C.P. King, and J. Lin, *Change in failure stress on the southern San Andreas fault system caused by the 1992 magnitude=7.4 Landers earthquake*, *Science* **258** (1992), 1328–1332.

- 
- [58] S. Toda, R.S. Stein, K. Richards-Dinger, and S. Bozkurt, *Forecasting the evolution of seismicity in Southern California: Animations built on earthquake stress transfer*, J. Geophys. Res. **110** (2005), B05S16.
- [59] T. Utsu, *A statistical study of the occurrence of aftershocks*, Geophysical Magazine **30** (1961), 521–605.
- [60] T. Utsu, *Representation and analysis of earthquake size distribution: a historical review and some new approaches*, Pure Appl. Geophys. **155** (1999), 509–535.
- [61] T. Utsu, Y. Ogata, and R.S. Matsu'ura, *The centenary of the Omori formula for a decay law of aftershock activity*, J. Phys. Earth **43** (1995), 1–33.
- [62] V. Vavryčuk, *Earthquake mechanisms and stress field*, Encyclopedia of earthquake engineering (M. Beer, I. A. Kougiumtzoglou, E. Patelli, and I. S.-K. Au, eds.), Springer-Verlag, Berlin, 2015.
- [63] D. J. Wald and T. H. Heaton, *Spatial and temporal distribution of slip for the 1992 Landers, California, earthquake*, Bull. Seismol. Soc. Am. **84** (1994), no. 3, 668–691.
- [64] M. Werner, M. Gerstenberger, M. Liukis, W. Marzocchi, D. Rhoades, M. Taroni, J. Zechar, C. Cattania, A. Christophersen, S. Hainzl, A. Helmstetter, A. Jiménez, S. Steacy, and T. Jordan, *Retrospective evaluation of time-dependent earthquake forecast models during the 2010-12 Canterbury, New Zealand, earthquake sequence*, Proceedings of the SSA Annual Meeting, Pasadena (USA), 2015.
- [65] J. Woessner and S. Wiemer, *Assessing the quality of earthquake catalogues: Estimating the magnitude of completeness and its uncertainty*, Bull. Seismol. Soc. Am. **95** (2005), no. 2, 684–698.
- [66] W. Yang, E. Hauksson, and P. M. Shearer, *Computing a large refined catalog of focal mechanisms for Southern California (1981-2010): Temporal stability of the style of faulting*, Bull. Seismol. Soc. Am. **102** (2012), 1179–1194.

## ACKNOWLEDGEMENTS

We are grateful to Álvaro González for some comments on the manuscript. The research leading to these results has received funding from “La Caixa” Foundation. V. N. acknowledges financial support from the Spanish Ministry of Economy and Competitive-

---

ness (MINECO, Spain), through the “María de Maeztu” Programme for Units of Excellence in R & D (Grant No. MDM-2014-0445). We also acknowledge financial support from MINECO under Grants No. FIS2015-71851-P and “Proyecto Redes de Excelencia” Grant No. MAT2015-69777-REDT. A. J. appreciates the hospitality of the Centre de Recerca Matemàtica.

#### **AUTHOR CONTRIBUTIONS STATEMENT**

V. N.-P. and A. J. performed the computations, A. J and A. C. wrote the manuscript. All authors discussed the results and reviewed the manuscript.